Coverage–Driven Electronic Decoupling of Fe–Phthalocyanine from a Ag(111) Substrate

6 AUTHORS, INCLUDING:

Gopakumar Thiruvancheril
Indian Institute of Technology Kanpur
29 PUBLICATIONS **525** CITATIONS

SEE PROFILE

Jörg Kröger
Technische Universität Ilmenau
99 PUBLICATIONS **2,013** CITATIONS

SEE PROFILE

Cormac Toher
Technische Universität Dresden
16 PUBLICATIONS **508** CITATIONS

SEE PROFILE

Gianaurelio Cuniberti
Technische Universität Dresden
293 PUBLICATIONS **4,663** CITATIONS

SEE PROFILE

Coverage-Driven Electronic Decoupling of Fe-Phthalocyanine from a Ag(111) Substrate

T. G. Gopakumar,*,[†] T. Brumme,[‡] J. Kröger,[§] C. Toher,[‡] G. Cuniberti,[‡] and R. Berndt[†]

[†]Institut für Experimentelle und Angewandte Physik, Christian-Albrechts-Universität zu Kiel, D-24098 Kiel, Germany

[‡]Institute for Materials Science and Max Bergmann Center of Biomaterials, Dresden University of Technology, D-01069 Dresden, Germany

[§]Institut für Physik, Technische Universität Ilmenau, D-98693 Ilmenau, Germany

Ⓢ Supporting Information

ABSTRACT: Coverage-dependent structural and electronic properties of Fe-phthalocyanine (FePc) molecules adsorbed on Ag(111) have been investigated by scanning tunneling microscopy/spectroscopy and density functional calculations. While spectra of single FePc molecules are dominated by a broad signature of Fe d orbitals, spectra of molecules in an ordered superstructure resolve spectroscopic contributions from individual d_{z^2} and d_{xz}/d_{yz} orbitals. Calculations suggest that an increased molecule−surface distance in the superstructure and a change of the Ag(111) surface electronic structure cause the spectral changes, which are consistent with a partial electronic decoupling of the molecules from the substrate. A progressive evolution toward a gap around the Fermi level is observed for molecules on the first and second molecular layer.
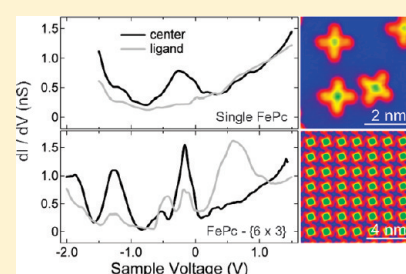
■ INTRODUCTION

The adsorption of organic molecules on a metal surface tends to change the molecular properties via electronic interactions, turning sharp electronic states into short-lived resonances. This may be detrimental to the functional properties the molecule exhibits in solution or in the gas phase. A number of approaches for tuning the molecule−substrate interaction have been reported. Thin spacer layers such as oxides,[1,2] alkali halides,[3−6] nitrides,[7] molecules,[8−11] or alkane buffer layers,[12−15] phenyladamantane,[8] and spacers within the molecule[16,17] have been used. Decoupling naturally occurs in multilayer films.[5,9,18−25] The degree of decoupling may be judged from the similarity of the molecular electronic structure to its pristine, vacuum state. The evolution of the electronic structure from submonolayer coverages to molecular multilayers has experimentally been investigated by, e.g., photoelectron spectroscopy.[18,19,26−29] Though scanning tunneling spectroscopy (STS) probes the electronic structure at a submolecular level, there have been very few previous reports on the evolution of the electronic structure of adsorbed molecules as a function of coverage.[9,18,25]

Here, we present a scanning tunneling microscopy (STM) and STS investigation of Fe-phthalocyanine (FePc) molecules on Ag(111). Molecules in single-layer islands exhibit significantly sharper molecular states, while spectra of single molecules only show a broad distribution of Fe d states. This surprising observation suggests a partial electronic decoupling of molecules from the surface without an intervening buffer layer. While changes may have been expected between the first and the second (or third) layer, no experimental data about the

decoupling right at the metal−organic interface are available. Concomitant density functional calculations indicate that the molecule−surface distance is increased in the superstructure, which explains the partial electronic decoupling. The trend toward decoupling continues with increasing distance of the molecule from the substrate. Molecules adsorbed on the first FePc layer exhibit some depletion of the local density of states around the Fermi energy, and molecules on top of the second layer exhibit a wide energy gap.

■ EXPERIMENT

Experiments were performed with a home-built scanning tunneling microscope operated at 7 K and in an ultrahigh vacuum with a base pressure of 10^{-9} Pa. Electrochemically etched W tips and Ag(111) surfaces were cleaned by Ar^+ bombardment and annealing. Molecules were evaporated from a heated Ta crucible and deposited onto Ag(111) at room temperature with a rate of ≈0.4 monolayers per minute as inferred from quartz microbalance readings and STM images. Spectroscopy of the differential conductance (dI/dV) was performed by superimposing a modulation (5−10 mV_{rms}, 7 kHz) on the sample voltage, V, and measuring the first harmonic of the current response with a lock-in amplifier.

■ THEORETICAL METHODS

Density functional calculations were performed with the PWscf code, which is part of the Quantum ESPRESSO package.[30] Calculations of the spin-resolved density of states of FePc molecules on a Ag(111) substrate were carried out using ultrasoft (Vanderbilt) pseudopotentials based on different approximations for the exchange-correlation energy together with a kinetic-energy cutoff of 25 Ry (1 Ry = 13.6 eV) for the plane wave basis set, the convergence of which has been checked with a higher cutoff of 35 Ry. The substrate was modeled using three layers of Ag in the (111) orientation with about 1.8 nm vacuum to the next periodically repeated layer. Using up to 6 Ag layers led to negligible changes in the electronic structure. The dimensions of the unit cell used for the simulation of a single FePc molecule on Ag(111) are 2.009 × 2.030 nm resulting in a 225-atom model. The ordered molecular superstructure (see definition below) was simulated by FePc molecules on Ag(111) arranged in periodically repeated cells with Fe–Fe distances of 1.45 and 1.51 nm along the long and short axes of the supercell, respectively. These distances are the smallest possible values which approximate the experimentally measured distances while maintaining a reasonable computational cost. Indeed, the simulation of the full superstructure would be computationally very expensive since the 18 FePc molecules alone without the surface would already contain 1026 atoms. An optimum geometry was obtained by relaxing the position of all atoms except for substrate atoms of the lowest Ag layer, whose coordinates were fixed to bulk positions. The self-consistent solution of the Kohn–Sham equations was obtained when the total energy changed by less than 10^{-6} Ry and the maximum force was less than 10^{-2} Ry Bohr^{-1} (1 Bohr = 0.529 nm). While the local density approximation (LDA) results in a molecule geometry that is comparable with the experiment, the entire molecule is strongly distorted if the generalized gradient approximation (GGA) is used. The central Fe atom is bonded to the surface, and the benzopyrrole groups move away from the surface. However, the LDA gives an incorrect ground state for bulk Fe,[31] and thus the electronic structure of a single Fe atom embedded in an organic ligand frame may be questionable as well. Therefore, we used the GGA together with a semiempirical approximation for the dispersion interactions as implemented in PWscf.[32,33] Taking into account phenomena such as van der Waals forces in this way has been shown to improve the agreement between experiment and calculations with respect to the geometry and the electronic properties for molecules on surfaces.[34-36] An artificial broadening of 0.005 Ry was used for the plots of the projected density of states (PDOS).

■ RESULTS AND DISCUSSION

Structural Properties. Figure 1 displays STM images of FePc molecules adsorbed on Ag(111) from isolated molecules [Figure 1a] over a closed layer [Figure 1b] to a two-layer film [Figure 1c]. Figure 1a clearly shows the typical cross-like shape of single phthalocyanine molecules adsorbed on metal surfaces. According to our calculations, the fully relaxed molecule adsorbs with its central Fe atom on a bridge position between two adjacent Ag atoms [Figure 1d, top view] and with its molecular plane parallel to the surface [Figure 1d, side view]. Furthermore, one pair of opposite benzopyrrole groups is aligned with a compact ⟨1$\bar{1}$0⟩ direction of Ag(111), which is in agreement with

the experimental observations and with previous studies of other metallophthalocyanines.[9,37,38] Over a range of voltages (−2, ..., 2 V) the molecules exhibit a bright center in constant-current STM images, which is due to Fe d orbitals according to our calculations and in agreement with earlier reports.[5,39−41] Upon increasing the coverage, the molecules arrange in an ordered superstructure. A geometrical model [Figure 1e] is proposed for the ordered layer based on experimental molecular lattice vectors, relative orientation of the molecule within the adlayer, and with respect to the substrate lattice. The supercell is indicated by a rectangle in Figure 1e, and its matrix notation reads

$$\begin{pmatrix} 29 & 0 \\ 8 & 16 \end{pmatrix}$$

As the unit cell contains {6 × 3} molecules, we refer to it for simplicity as the {6 × 3} structure. The direction of the longer supercell axis coincides with a ⟨1$\bar{1}$0⟩ direction. One of the molecular axes along the ligands encloses an angle of 30° with this supercell direction, which minimizes steric hindrance between adjacent molecules. The distances between adjacent molecular centers are (1.39 ± 0.03) nm and (1.34 ± 0.03) nm along the long and short supercell axes, respectively. Upon further increase of the coverage, the first molecular layer is first closed and exhibits a surface density of molecules, which is ≈13% higher than in the {6 × 3} structure. Then, molecules start to occupy sites on the first and second layer [labeled I and II in Figure 1c]. A similar Stranski–Krastanov-type growth has recently been reported for SnPc on Au(111).[6] The unit cell of the ordered second layer (not shown) is a rhomboid with side lengths of (1.35 ± 0.03) nm and (1.25 ± 0.03) nm and an angle of (83 ± 2)° enclosed by the unit cell vectors. As is evident from STM images [Figure 1c], the molecular plane is tilted with respect to the surface normal. The tilted adsorption configuration enables a favorable interaction between the π electron systems of adjacent molecules [Figure 1f].[23,42] The ordered monolayers as well as the π stacking in higher molecular layers have been observed for a variety of phthalocyanine molecules.[6,9,20,43,44,74]

Electronic Properties. The evolution of the electronic structure with coverage has been investigated by dI/dV spectroscopy. In Figure 2a spectra acquired from the center (black) and the ligands (gray) of a single FePc adsorbed to Ag(111) are compared. Spectra of the FePc center are dominated by a broad feature centered at ≈ −0.25 V. Additional weak shoulders are observed at ≈ −1.25, ≈ −0.60, and ≈ −0.05 V. Spectra acquired from the ligands are rather featureless except for a broad signature at ≈0.60 V. The single-molecule spectra of Figure 2a are very similar to spectra of phthalocyanine molecules with other magnetic centers.[45−48] The spatial distribution of the molecular orbitals at −1.25, −0.25, and 0.60 V may be obtained from constant-current maps of dI/dV [Figure 2c] recorded at these voltages. The dI/dV maps acquired at −1.25 and −0.25 V show a dominant contribution at the center of the molecule as expected for the Fe d state observed at these voltages in the dI/dV spectra [Figure 2a]. dI/dV maps at 0.60 V exhibit additional spectral weight at the ligands. dI/dV maps have been corrected for tip displacements during measurement according to reference.[49]

A remarkable change of the spectra of individual molecules is observed upon forming the {6 × 3} structure [Figure 2b].

B

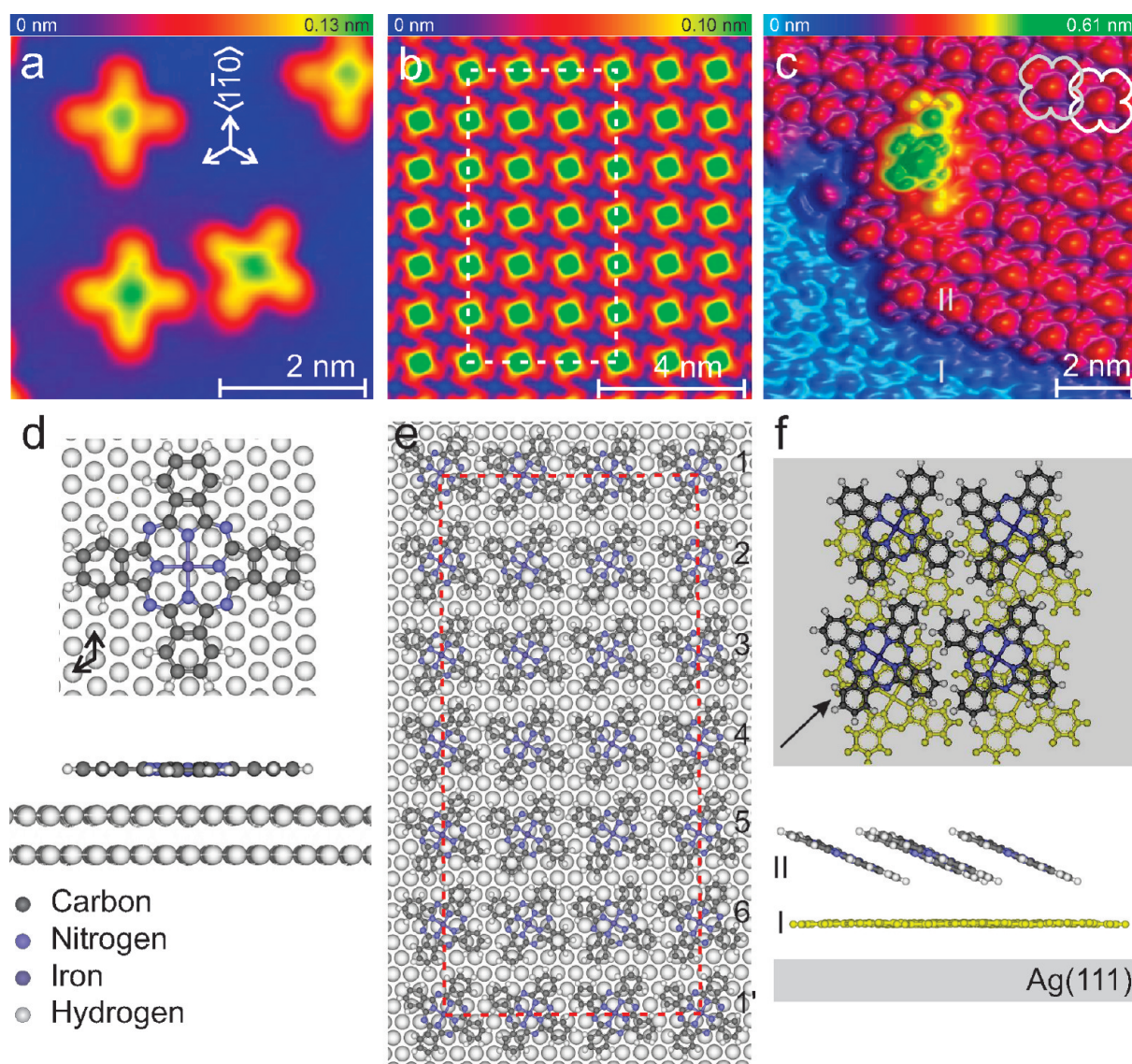dx.doi.org/10.1021/jp2038619 |*J. Phys. Chem. C* XXXX, XXX, 000–000

Figure 1. Constant-current STM images of (a) single FePc molecules on Ag(111) (0.45 V, 100pA), (b) the {6 × 3} structure of FePc on Ag(111) (−1.3 V, 100pA) with indicated unit cell (dashed line), and (c) FePc molecules adsorbed on the first (I) and second (II) molecular layer (2 V, 100 pA) displayed in a pseudothree-dimensional presentation. (d) Top and side view of calculated fully relaxed FePc adsorption geometry. The central Fe atom resides at a Ag(111) bridge site. One pair of opposite ligands is oriented along a crystallographic direction. (e) Sketch of the {6 × 3} structure with indicated unit cell (dashed line). (f) Top and side view of adsorption configuration in the first (I) and second (II) molecular layer on Ag(111) (gray); arrow in the upper panel indicates the direction along which the side view is shown.

Well-resolved features appear at voltages where only weak signals are present in spectra of isolated molecules [Figure 2a]. In particular, the broad peak at ≈ −0.25 V in single-molecule spectra becomes sharper and shifts to ≈ −0.17 V in the {6 × 3} structure [arrows in Figure 2a,b]. Possible shifts of the other features are difficult to discern as they correspond to rather weak shoulders in the single-molecule spectrum [Figure 2a]. A contamination of the probe by accidentally attached molecules is unlikely to be at the origin of the observations. On pristine Ag(111) areas the spectroscopic signature of the Shockley-type surface state has been observed with the same tip that has been used for spectroscopy of molecules in the {6 × 3} structure. A comparison of the spectra in Figure 2a,b reveals that the positions of the weak shoulders (≈ −1.25 V, −0.6 V, 0.6 V) in the single-molecule spectra approximately coincide with those of the peaks

in the spectra of molecules in the {6 × 3} structure. Therefore, we conclude that the orbital contributions to dI/dV data are already present in the single-molecule spectra, albeit to a smaller extent than observed from the superstructure. Repeated experiments showed the reproducibility of the shoulder-like features in the spectra.

The experimental spectra give rise to several questions such as: Which molecular orbital induces which peak in dI/dV spectra? Why does the electronic structure of FePc molecules evolve in the peculiar way upon forming the superstructure? Which mechanism is at the origin of the shift of spectral features? These questions may be answered by considering the calculated PDOS of d orbitals of the central Fe atom. When recording spectra above the center of the molecule, the tip is closest to the central Fe atom. We therefore focus on the Fe d orbitals and particularly

C

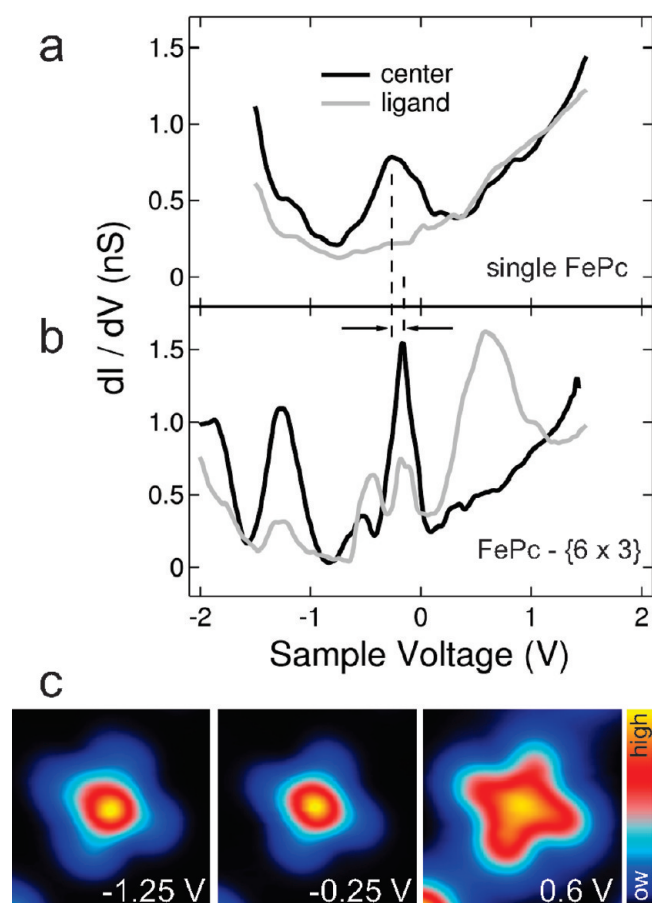dx.doi.org/10.1021/jp2038619 |*J. Phys. Chem. C* XXXX, XXX, 000–000

Figure 2. Averaged constant-height dI/dV spectra acquired from the center (black) and the ligands (gray) of (a) single molecules and (b) molecules embedded in the $\{6 \times 3\}$ structure (feedback loop parameters: 1.5 V, 1 nA). The ligand spectrum in (b) is multiplied by a factor of 2.5 for clarity of small features. The dashed lines indicate a peak shift of ≈ 0.08 V toward positive voltages upon forming the $\{6 \times 3\}$ structure. (c) Constant-current maps of dI/dV acquired at indicated voltages.

Figure 3. Calculated projected density of states (PDOS) of Fe d orbitals of (a) a single fully relaxed FePc molecule on Ag(111) and (b) a fully relaxed FePc in the simulated $\{6 \times 3\}$ structure on Ag(111) [shaded area: full PDOS, lines: d_{z^2} (black), d_{xz}/d_{yz} (red), $d_{xy}/d_{x^2-y^2}$ (blue)]. Owing to the plane wave description of molecular states, the depicted projected density of states contains ligand states, albeit to a small extent.

Table 1. Comparison of Experimental (exp) and Calculated (calc) Orbital Energies and Its Dominant Orbital Character of a FePc Molecule in the $\{6 \times 3\}$ Structure on Ag(111)

E^{exp} (eV)	E^{calc} (eV)	orbital character
−1.25	−1.60	d_{xz}/d_{yz}
−0.60	−0.65	d_{z^2}
−0.17	−0.22	d_{xz}/d_{yz}
−0.05	−0.05	d_{z^2}
0.60	0.80	d_{xz}/d_{yz}, d_{z^2}

discuss d_{z^2} and d_{xz}/d_{yz} Fe orbitals which essentially determine the shape and position of the experimental peaks, with a negligible influence of the $d_{xy}/d_{x^2-y^2}$ states. This approach is similar to earlier work on CoPc and CuPc on Au(111).[50] It reflects the symmetry of d_{z^2} and d_{xz}/d_{yz} orbitals and their large extension out of the molecular plane.[50] Due to the plane wave basis set used for the description of molecular states, the PDOS contains contributions of ligand states as well. However, these contributions are weak, and calculations reveal that variations of the density of states at the Fermi energy are dominated by Fe d orbitals.

Figure 3 shows the total PDOS of Fe d orbitals of a single FePc on Ag(111) [Figure 3a] and of FePc embedded in the $\{6 \times 3\}$ superstructure on Ag(111) [Figure 3b] as a shaded area. Individual contributions to the total PDOS from Fe d_{z^2}, Fe d_{xz}/d_{yz}, and Fe $d_{xy}/d_{x^2-y^2}$ orbitals appear as lines with different colors. Obviously, the calculated spectral features appear sharper than their experimental counterparts, which results from showing only the contributions of Fe d orbitals. The inclusion of Ag s states leads to a broadening of calculated signatures. An extension of the calculations to silver s states can be found in the Supporting Information, S1. On the basis of the calculated data presented in Figure 3,
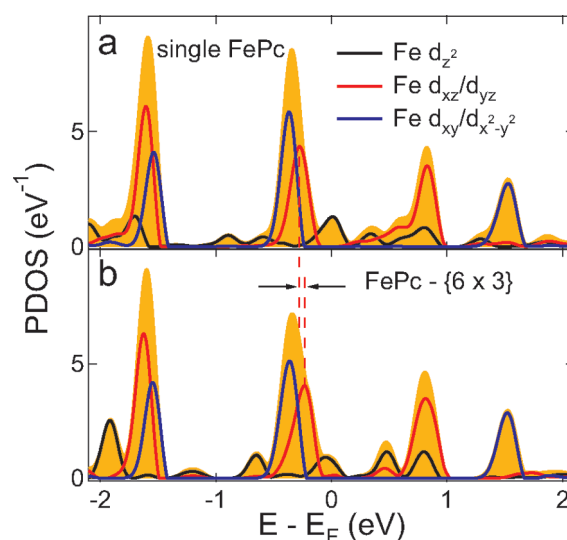
the experimentally observed shoulders and peaks at ≈ -0.60 V are due to the d_{z^2} orbitals of the central Fe atom, while the spectroscopic features at ≈ -0.25 and at ≈ -0.17 V observed from a single FePc and a FePc in the $\{6 \times 3\}$ superstructure, respectively, are composed of contributions from d_{xz}/d_{yz} orbitals. The weak shoulder at ≈ -0.05 V has essentially d_{z^2} character. At ≈ -1.25 V contributions from d_{xz}/d_{yz} orbitals play the dominant role, whereas the shoulder and peak at ≈ 0.60 V are due to d_{xz}/d_{yz} and d_{z^2} orbitals. Experimental and calculated peak positions together with orbital characters are summarized in Table 1. For unoccupied states ($V > 0$), the calculated PDOS deviates strongly from experimental data, which is due to the inability of ground state density functional theory to accurately describe unoccupied states.[51]

The calculations indicate a possible origin of the experimentally observed peak shift between a single FePc [≈ -0.25 V, Figure 2a] and FePc in the $\{6 \times 3\}$ structure [≈ -0.17 V, Figure 2b]. According to the simulations, FePc molecules embedded in the $\{6 \times 3\}$ structure exhibit an adsorption height that is ≈ 5 pm higher than the adsorption height of a single FePc on Ag(111). The average adsorption height in the experiments may be even higher since molecules also occupy on-top sites and the calculated molecule−surface distance for these sites is higher than in the bridge configuration. These different adsorption heights

induce a shift of the calculated d_{xz}/d_{yz} state near ≈ -0.27 eV for a single FePc to ≈ -0.22 eV for a FePc in the superstructure. The calculated shift of $\delta \approx 0.05$ eV (indicated by dashed lines in Figure 3) is comparable with the experimental shift of ≈ 0.08 eV. The calculated shift of $d_{xy}/d_{x^2-y^2}$ orbital energies toward higher values is, however, much smaller than the one of the d_{xz}/d_{yz} orbitals because of the negligible hybridization of the molecular in-plane states with the Ag(111) electronic continuum. The shift of the d_{xz}/d_{yz} orbital energies shows a reverse chemisorption process, which is indicative of a weakening of the molecule−surface hybridization in the $\{6 \times 3\}$ structure. The calculations show that the adsorption energy of each FePc molecule in the $\{6 \times 3\}$ structure is ≈ 213 meV lower than the adsorption energy of a single FePc molecule on Ag(111), which is additional evidence for a weakening of the molecule−surface interaction (see Supporting Information, S2). The adsorption energies calculated for FePc are comparable with literature values.[37,52] Furthermore, calculations for a free-standing $\{6 \times 3\}$ layer reveal a strong molecule−molecule interaction [absence of Ag(111), Supporting Information, S3]. Moreover, the decreased FePc−Ag(111) coupling can likewise be inferred from the evolution of the Fe d_{z^2} orbital, where the splitting into bonding and antibonding states is reduced. Indeed, calculated Fe d_{z^2} energies exhibit a shift from −1.90 eV for single FePc molecules to −1.95 eV for FePc molecules embedded in the $\{6 \times 3\}$ superstructure. These orbitals tend to move toward their gas-phase energies, which are well below the Fermi level. A shift of molecular orbitals owing to different intermolecular coupling in different phases of perylenetetracarboxylic-dianhydride has previously been reported to be ≈ 0.35 eV.[53]

An additional hint to the origin of the sharpening of spectroscopic signatures upon forming the $\{6 \times 3\}$ structure is provided by the behavior of the Ag(111) s states. The calculations show that the s states of the surface atoms are rather broad underneath a single FePc molecule, which contributes to the width of the spectral features observed in the experiments. The molecular superstructure, which may be viewed as a periodic mesh of scattering centers, modifies the electronic states of the substrate. In the simulated superstructure, the s states are sharper, and their energies coincide with those of the Fe d_{z^2} orbitals of the molecules. Further detail may be found in the Supporting Information, S1.

Next, variations of the electronic states observed from different molecules within the superstructure are presented. Figure 4 shows spectra from a row of molecules along the long axis of the supercell. The data were recorded above those benzene rings which are oriented along the $\langle 1\bar{1}0 \rangle$ direction. Molecules are numbered according to the scheme introduced in Figure 1e. The similarity of the spectra from Molecules 1 and 1′ indicates the reproducibility of the measurements. The spectroscopic signature of the d_{z^2} orbital at ≈ 0.60 V is broad at Molecules 1 and 1′ and evolves into a more peak-shaped structure toward the center of the unit cell (Molecule 4). The broad feature of Molecule 1 is reminiscent of the spectrum of an isolated molecule [Figure 2a].

Although the $\{6 \times 3\}$ structure is too large to be treated by the calculations, the simulation of a single FePc on Ag(111) provides a hint to an interpretation of the experimental data. As single molecules adsorb with their Fe atom at a bridge site, we assume that Molecule 1 of the superstructure is also located at a bridge position. According to the model structure in Figure 1e, Molecules 2, 3 and 5, 6 reside between bridge sites, while Molecule 4
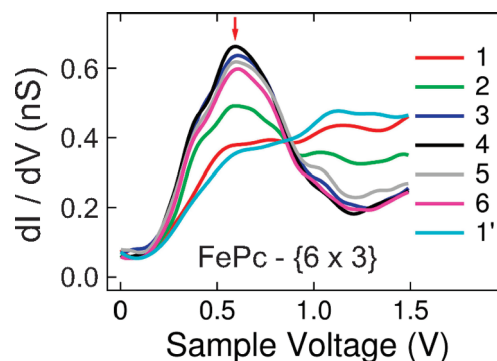

Figure 4. Constant-height dI/dV spectra (feedback loop parameters: 1.5 V, 1 nA) acquired at ligands of Molecules 1 to 1′ indicated in Figure 1e.

adopts again a bridge site. The dI/dV spectrum of Molecule 4, however, is not similar to the spectra of Molecules 1 and 1′. Compared to Molecules 1 and 1′, which exhibit an opposite ligand pair residing *atop* a compact Ag(111) atom row, the corresponding ligand pair of Molecule 4 resides *between* two compact Ag(111) rows. This different adsorption geometry is most likely the origin of the dissimilar dI/dV spectra. A weak modulation of the ligand electronic structure is also observed along the short axis of the $\{6 \times 3\}$ structure (not shown). This observation may reflect small changes of the adsorption positions along this axis. Modifications of the molecular electronic structure depending on the adsorption site have been reported for a variety of molecules.[19,48,54−57]

STS data of molecules adsorbed on top of the first and second molecular layers are presented in Figure 5. While the spectra have been acquired at the benzene ligands, data recorded above the Fe centers may be found in the Supporting Information, S4. We attribute the features at ≈ -1.2 V and ≈ 0.36 V [Figure 5a] and at ≈ -1.2 V and ≈ 0.92 V [Figure 5b] to the spectroscopic signatures of the highest occupied molecular orbital (HOMO) and the lowest unoccupied molecular orbital (LUMO), respectively. The weaker structure at ≈ -0.43 V in the second-layer spectrum is most likely due to an interface state. It cannot be discerned anymore in the third-layer data. Compared to spectra of molecules in the $\{6 \times 3\}$ structure [Figure 2b], the differential conductance between the HOMO- and LUMO-related spectroscopic features is reduced in the second-layer spectra. In third-layer spectra, the gap is well developed and is ≈ 2.1 eV, which is comparable with the experimentally observed optical[58] and transport[59] gap. The calculated HOMO−LUMO gap width for a gas-phase molecule, however, is lower than the experimental values.[60]

Besides the evolution of an energy gap between HOMO and LUMO, a comparison of second-layer and third-layer spectra reveals a shift of unoccupied orbitals to higher energies. The peaks labeled A, B, and C in Figure 5a shift from 0.36, 0.61, and 1.09 V in the second-layer spectrum to 0.92, 1.24, and 1.67 V, which are the voltages of peaks A′, B′, and C′ in the third-layer spectrum [Figure 5b]. The voltage differences are 0.56, 0.63, and 0.58 V for the peak pairs AA′, BB′, and CC′, respectively. Two contributions to the observed shifts have been considered. First, a voltage drop may occur over the FePc film. To estimate the voltage drop, a simple model of a plate capacitor partly filled with a dielectric has been used.[61,62] The voltage drop over the
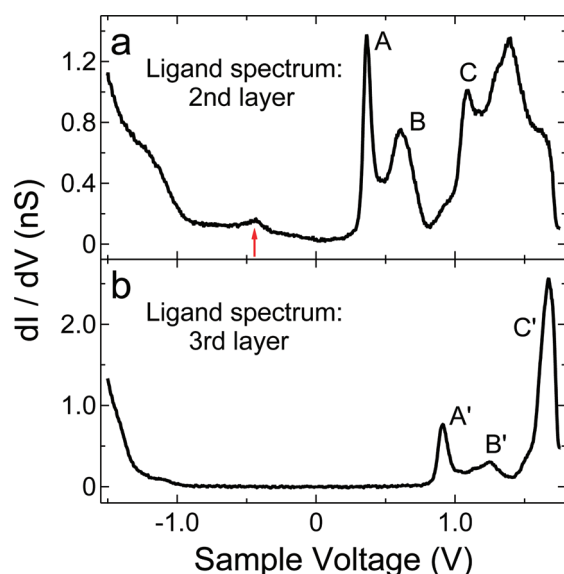
E

Figure 5. Constant-height dI/dV spectra of FePc ligands adsorbed on the (a) first and (b) second molecular layer (feedback loop parameters: 1.75 V, 1 nA). The arrow in (a) indicates the position of a molecule—surface hybrid state at ≈ -0.43 V. Peaks labeled A, B, and C in (a) and A′, B′, and C′ in (b) indicate pairs of peaks, which shift by similar magnitudes, i.e., from ≈ 0.36 (A) to ≈ 0.92 V (A′), from ≈ 0.61 (B) to ≈ 1.24 V (B′), and from ≈ 1.09 (C) to ≈ 1.67 V (C′).

dielectric (thickness d, dielectric constant ε) can be readily calculated as $V/(\varepsilon z/d + 1)$ with z being the width of the vacuum gap. Calculated values of the CuPc dielectric constant[63] vary between 10 and 20 and have been used for the estimate because of the lack of corresponding data for FePc. From constant-current STM images the thickness of three layers of FePc is $d \approx$ 0.66 nm. The tip—molecule distance has been estimated by the displacement of the tip which is required to contact the molecule ($z \approx 0.45$ nm).[64] With these values and a sample voltage of $V =$ 1 V, voltage drops between 70 and 130 mV are obtained. Within this model the peak shift between the second and third layer is even lower. However, since contact experiments on the second layer were hardly reproducible, an estimate of the tip—molecule distance for this layer is not available. A second contribution to the shift may originate from screening effects due to the polarizable neighborhood of the molecule or due to image charges in the metal substrate.[65−69] Since a molecule in the third molecular layer is similarly coordinated as a molecule in the second layer, we do not consider screening by neighboring molecules. Indeed, the screening by nearby molecules is proportional to the inverse fourth power of the intermolecular distance.[25,70−72] The molecule—surface distances, however, are different for molecules in the second (≈ 0.41 nm) and the third (≈ 0.66 nm) layer as extracted from apparent heights in constant-current STM images. These values give rise to an interplanar distance of ≈ 0.25 nm. The apparent heights need not necessarily coincide with actual geometric dimensions. Therefore, STM data have been compared with X-ray diffraction data obtained from crystalline FePc,[73] which provide a FePc interplanar distance of 0.34 nm.[73] The screening due to image charges in the metal can be modeled according to $e^2/(8\pi\varepsilon_0 R)$ (e, electron charge; ε_0, vacuum permittivity; R, molecule—surface distance).[25,67,72] Using the STM-derived interplanar FePc distance, a difference of the screening of ≈ 670 meV has been extracted, while the

interplanar distance of ≈ 0.34 nm for FePc[73] results in a difference of the screening between the second and third layer of ≈ 400 meV. As a consequence, the screening effect appears to play the major role in the observed shift.

CONCLUSION

A partial electronic decoupling of FePc molecules on Ag(111) has been achieved in an ordered superstructure. Density functional calculations reveal that in the superstructure the intermolecular interactions are increased at the expense of the molecule—surface coupling, which is accompanied by an increased molecule—surface distance. Since no complex spacers are needed the results clearly show that a variation of the adsorption height determines the coupling between the molecule and surface. The coverage-driven effective decoupling of FePc from the metal within the first layer and the evolution of electronic structure are likely to occur for other adsorbed molecules.

ASSOCIATED CONTENT

Ⓢ Supporting Information. (S1) Projected density of states of Fe s and Ag(111) s states, (S2) adsorption energies, (S3) density of states of single FePc and FePc embedded in a $\{6 \times 3\}$ structure in vacuum, and (S4) spectra of dI/dV of the FePc center in the second and third molecular layers. This material is available free of charge via the Internet at http://pubs.acs.org.

AUTHOR INFORMATION

Corresponding Author
*E-mail: gopa@physik.uni-kiel.de. Phone: +494318803865. Fax: +494318802510.

ACKNOWLEDGMENT

REFERENCES

(1) Qiu, X. H.; Nazin, G. V.; Ho, W. *Science* **2003**, *299*, 542.
(2) Heinrich, A. J.; Gupta, J. A.; Lutz, C. P.; Eigler, D. M. *Science* **2004**, *306*, 466.
(3) Ćavar, E.; Blüm, M.-C.; Pivetta, M.; Patthey, F.; Chergui, M.; Schneider, W.-D. *Phys. Rev. Lett.* **2005**, *95*, 196102.
(4) Repp, J.; Meyer, G.; Paavilainen, S.; Olsson, F. E.; Persson, M. *Phys. Rev. Lett.* **2005**, *95*, 225503.
(5) Scarfato, A.; Chang, S.-H.; Kuck, S.; Brede, J.; Hoffmann, G.; Wiesendanger, R. *Surf. Sci.* **2008**, *602*, 677.
(6) Wang, Y. F.; Kröger, J.; Berndt, R.; Tang, H. *J. Am. Chem. Soc.* **2010**, *132*, 12546.
(7) Hirjibehedin, C. F.; Lutz, C. P.; Heinrich, A. J. *Science* **2006**, *312*, 1021.
(8) Franke, K. J.; Schulze, G.; Henningsen, N.; Fernández-Torrente, I.; Pascual, J. I.; Zarwell, S.; Rück-Braun, K.; Cobian, M.; Lorente, N. *Phys. Rev. Lett.* **2008**, *100*, 036807.
(9) Wang, Y. F.; Kröger, J.; Berndt, R.; Hofer, W. A. *Angew. Chem., Int. Ed.* **2009**, *48*, 1261.

(10) Wang, Y. F.; Kröger, J.; Berndt, R.; Hofer, W. A. *J. Am. Chem. Soc.* **2009**, *131*, 3639.

(11) Cheng, Z. H.; Du, S. X.; Jiang, N.; Zhang, Y. Y.; Guo, W.; Hofer, W. A.; Gao, H.-J. *Surf. Sci.* **2011**, *605*, 415.

(12) Staub, R.; Toerker, M.; Fritz, T.; Schmitz-Hübsch, T.; Sellam, F.; Leo, K. *Surf. Sci.* **2000**, *445*, 368.

(13) Xu, B.; Yin, S.; Wang, C.; Qiu, X.; Zeng, Q.; Bai, C. *J. Phys. Chem. B* **2000**, *104*, 10502.

(14) Cyganik, P.; Buck, M.; Azzam, W.; Wöll, C. *J. Phys. Chem. B* **2004**, *108*, 4989.

(15) Zhao, J.; Zeng, C.; Cheng, X.; Wang, K.; Wang, G.; Yang, J.; Hou, J. G.; Zhu, Q. *Phys. Rev. Lett.* **2005**, *95*, 045502.

(16) Langlais, V. J.; Schlittler, R. R.; Tang, H.; Gourdon, A.; Joachim, C.; Gimzewski, J. K. *Phys. Rev. Lett.* **1999**, *83*, 2809.

(17) Ge, X.; Kuntze, J.; Berndt, R.; Tang, H.; Gourdon, A. *Chem. Phys. Lett.* **2008**, *458*, 161.

(18) Tsiper, E. V.; Soos, Z. G.; Gao, W.; Kahn, A. *Chem. Phys. Lett.* **2002**, *360*, 47.

(19) Berner, S.; de Wild, M.; Ramoino, L.; Ivan, S.; Baratoff, A.; Güntherodt, H.-J.; Suzuki, H.; Schlettwein, D.; Jung, T. A. *Phys. Rev. B* **2003**, *68*, 115410.

(20) Takada, M.; Tada, H. *Chem. Phys. Lett.* **2004**, *392*, 265.

(21) Braun, D.; Schirmeisen, A.; Fuchs, H. *Surf. Sci.* **2005**, *575*, 3.

(22) Nicoara, N.; Román, E.; Gómez-Rodríguez, J. M.; Martín-Gago, J. A.; Méndez, J. *Org. Electron.* **2006**, *7*, 287.

(23) Gopakumar, T. G.; Müller, F.; Hietschold, M. *J. Phys. Chem. B* **2006**, *110*, 6051.

(24) Gustafsson, J. B.; Zhang, H. M.; Johansson, L. S. O. *Phys. Rev. B* **2007**, *75*, 155414.

(25) Wang, Y.; Yamachika, R.; Wachowiak, A.; Grobis, M.; Crommie, M. F. *Nat. Mater.* **2008**, *7*, 194.

(26) Peisert, H.; Petershans, A.; Chassé, T. *J. Phys. Chem. C* **2008**, *112*, 5703.

(27) Häming, M.; Scheuermann, C.; Schöll, A.; Reinert, F.; Umbach, E. *J. Electron Spectrosc. Relat. Phenom.* **2009**, *174*, 59.

(28) Gorgoi, M.; Zahn, D. *Org. Electron.* **2005**, *6*, 168.

(29) Schwieger, T.; Peisert, H.; Knupfer, M. *Chem. Phys. Lett.* **2004**, *384*, 197.

(30) PWscf is part of the QUANTUM-ESPRESSO package distributed by Baroni, S.; DalCorso, A.; de Gironcoli, S.; Giannozzi, P.; Cavazzoni, C.; Ballabio, G.; Scandolo, S.; Chiarotti, G.; Focher, P.; Pasquarello, A.; Laasonen, K.; Trave, A.; Car, R.; Marzari, N.; Kokalj, A. (http://www.pwscf.org).

(31) Leung, T. C.; Chan, C. T.; Harmon, B. N. *Phys. Rev. B* **1991**, *44*, 2923.

(32) Grimme, S. *J. Comput. Chem.* **2006**, *27*, 1787.

(33) Barone, V.; Casarin, M.; Forrer, D.; Pavone, M.; Sambi, M.; Vittadini, A. *J. Comput. Chem.* **2009**, *30*, 934.

(34) McNellis, E.; Meyer, J.; Reuter, K. *Phys. Rev. B* **2009**, *80*, 205414.

(35) Rohlfing, M.; Bredow, T. *Phys. Rev. Lett.* **2008**, *101*, 266106.

(36) Romaner, L.; Nabok, D.; Puschnig, P.; Zojer, E.; Ambrosch-Draxl, C. *New J. Phys.* **2009**, *11*, 053010.

(37) Heinrich, B. W.; Iacovita, C.; Brumme, T.; Choi, D.-J.; Limot, L.; Rastei, M. V.; Hofer, W. A.; Kortus, J.; Bucher, J.-P. *J. Phys. Chem. Lett.* **2010**, *1*, 1517.

(38) Iacovita, C.; Rastei, M. V.; Heinrich, B. W.; Brumme, T.; Kortus, J.; Limot, L.; Bucher, J. P. *Phys. Rev. Lett.* **2008**, *101*, 116602.

(39) Åhlund, J.; Schnadt, J.; Nilson, K.; Göthelid, E.; Schiessling, J.; Besenbacher, F.; Mårtensson, N.; Puglia, C. *Surf. Sci.* **2007**, *601*, 3661.

(40) Gao, L.; Ji, W.; Hu, Y. B.; Cheng, Z. H.; Deng, Z. T.; Liu, Q.; Jiang, N.; Lin, X.; Guo, W.; Du, S. X.; Hofer, W. A.; Xie, X. C.; Gao, H.-J. *Phys. Rev. Lett.* **2007**, *99*, 106402.

(41) Takami, T.; Carrizales, C.; Hipps, K. *Surf. Sci.* **2009**, *603*, 3201.

(42) Hunter, C. A.; Sanders, J. K. M. *J. Am. Chem. Soc.* **1990**, *112*, 5525.

(43) Hipps, K. W.; Lu, X.; Wang, X. D.; Mazur, U. *J. Phys. Chem.* **1996**, *100*, 11207.

(44) Suto, K.; Yoshimoto, S.; Itaya, K. *J. Am. Chem. Soc.* **2003**, *125*, 14976.

(45) Zhao, A.; Li, Q.; Chen, L.; Xiang, H.; Wang, W.; Pan, S.; Wang, B.; Xiao, X.; Yang, J.; Hou, J. G.; Zhu, Q. *Science* **2005**, *309*, 1542.

(46) Kröger, J.; Jensen, H.; Néel, N.; Berndt, R. *Surf. Sci.* **2007**, *601*, 4180.

(47) Takada, M.; Tada, H. *Jpn. J. Appl. Phys.* **2005**, *44*, 5332.

(48) Gopakumar, T. G.; Néel, N.; Kröger, J.; Berndt, R. *Chem. Phys. Lett.* **2009**, *484*, 59.

(49) Ziegler, M.; Néel, N.; Sperl, A.; Kröger, J.; Berndt, R. *Phys. Rev. B* **2009**, *80*, 125402.

(50) Lu, X.; Hipps, K. W.; Wang, X. D.; Mazur, U. *J. Am. Chem. Soc.* **1996**, *118*, 7197.

(51) Cohen, A. J.; Mori-Sánchez, P.; Yang, W. *Science* **2008**, *321*, 792.

(52) Casarin, M.; Marino, M. D.; Forrer, D.; Sambi, M.; Sedona, F.; Tondello, E.; Vittadini, A.; Barone, V.; Pavone, M. *J. Phys. Chem. C* **2010**, *114*, 2144.

(53) Kröger, J.; Jensen, H.; Berndt, R.; Rurali, R.; Lorente, N. *Chem. Phys. Lett.* **2007**, *438*, 249.

(54) Rogero, C.; Pascual, J. I.; Gómez-Herrero, J.; Baró, A. M. *J. Chem. Phys.* **2001**, *116*, 832.

(55) Li, H. I.; Franke, K. J.; Pascual, J. I.; Bruch, L. W.; Diehl, R. D. *Phys. Rev. B* **2009**, *80*, 085415.

(56) Martínez-Blanco, J.; Klingsporn, M.; Horn, K. *Surf. Sci.* **2010**, *604*, 523.

(57) Auwärter, W.; Seufert, K.; Klappenberger, F.; Reichert, J.; Weber-Bargioni, A.; Verdini, A.; Cvetko, D.; Dell'Angela, M.; Floreano, L.; Cossaro, A.; Bavdek, G.; Morgante, A.; Barth, J. V. *Phys. Rev. B* **2010**, *81*, 245403.

(58) Kumar, G. A.; Thomas, J.; George, N.; Unnikrishnan, N. V.; Radhakrishnan, P.; Nampoori, V. P. N.; Vallabhan, C. P. G. *J. Mater. Sci.* **2000**, *35*, 2539.

(59) Sharma, G. D.; Kumar, R.; Roy, M. S. *Sol. Energy Mater. Sol. Cells* **2006**, *90*, 32.

(60) Liu, Z.; Zhang, X.; Zhang, Y.; Jiang, J. *Spectrochim. Acta A* **2007**, *67*, 1232.

(61) Guisinger, N. P.; Yoder, N. L.; Hersam, M. C. *Proc. Natl. Acad. Sci.* **2005**, *102*, 8838.

(62) Matino, F.; Schull, G.; Köhler, F.; Gabutti, S.; Mayor, M.; Berndt, R. *Proc. Natl. Acad. Sci.* **2010**, *108*, 961.

(63) Ramprasad, R.; Shi, N. *Appl. Phys. Lett.* **2006**, *88*, 222903.

(64) Kröger, J.; Néel, N.; Sperl, A.; Wang, Y. F.; Berndt, R. *New J. Phys.* **2009**, *11*, 125006.

(65) Lang, N. D.; Kohn, W. *Phys. Rev. B* **1973**, *7*, 3541.

(66) Zaremba, E.; Kohn, W. *Phys. Rev. B* **1976**, *13*, 2270.

(67) Hesper, R.; Tjeng, L. H.; Sawatzky, G. A. *Europhys. Lett.* **1997**, *40*, 177.

(68) Ischii, H.; Sugiyama, K.; Ito, E.; Seki, K. *Adv. Mater.* **1999**, *11*, 605.

(69) Koch, N.; Kahn, A.; Ghijsen, J.; Pireaux, J.-J.; Schwartz, J.; Johnson, R. L.; Elschner, A. *Appl. Phys. Lett.* **2003**, *82*, 70.

(70) Lof, W. R.; Vanveenendaal, M. A.; Koopmans, B.; Jonkman, H. T.; Sawatzky, G. A. *Phys. Rev. Lett.* **1992**, *68*, 3924.

(71) Bonin, K. D.; Kresin, V. V. *Electric-Dipole Polarizabilities of Atoms, Molecules, and Clusters*; World Scientific: Singapore, 1997.

(72) Torrente, I. F.; Franke, K. J.; Pascual, J. I. *J. Phys.: Condens. Matter* **2008**, *20*, 184001.

(73) Evangelisti, M.; Bartolomé, J.; de Jongh, L. J.; Filoti, G. *Phys. Rev. B* **2002**, *66*, 144410.

(74) Böhringer, M.; Berndt, R.; Schneider, W.-D. *Phys. Rev. B* **1997**, *55*, 1384.